AD-A063 159 NAVAL RESEARCH LAB WASHINGTON D C F/G 17/2.1
METEORBURST COMMUNICATION SYSTEMS: ANALYSIS AND SYNTHESIS.(U)
DEC 78 A E SPEZIO
UNCLASSIFIED NRL-8286 NL

| OF |
AD
A063159

END
DATE
FILMED
3-79
DDC

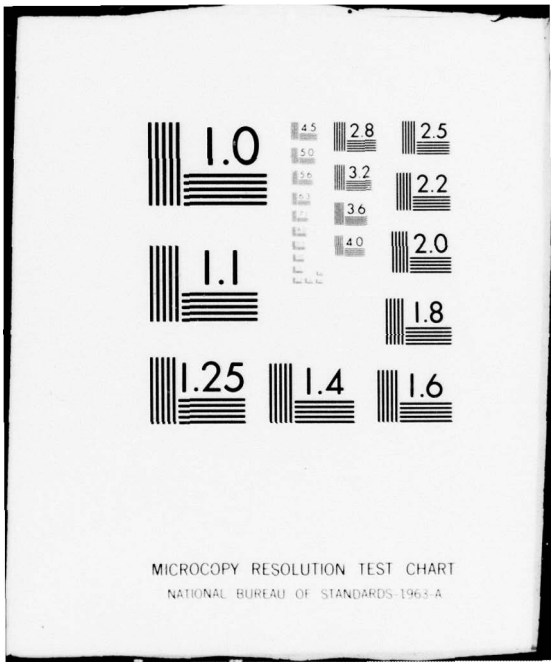
1.0
1.1
1.25
1.4
1.6
2.8
3.2
3.6
4.0
2.5
2.2
2.0
1.8
MICROCOPY RESOLUTION TEST CHART
NATIONAL BUREAU OF STANDARDS-1963-A

LEVEL II (12) B.S.

NRL Report 8286

Meteor-Burst Communication Systems: Analysis and Synthesis

ANTHONY E. SPEZIO

EW Support Measures Branch
Tactical Electronic Warfare Division

December 28, 1978

NAVAL RESEARCH LABORATORY
Washington, D.C.

SECURITY CLASSIFICATION OF THIS PAGE *(When Data Entered)*

REPORT DOCUMENTATION PAGE

READ INSTRUCTIONS BEFORE COMPLETING FORM

1. REPORT NUMBER: NRL Report 8286	2. GOVT ACCESSION NO.
3. RECIPIENT'S CATALOG NUMBER	
4. TITLE *(and Subtitle)*: METEOR-BURST COMMUNICATION SYSTEMS: ANALYSIS AND SYNTHESIS	5. TYPE OF REPORT & PERIOD COVERED: Final report on one phase of a continuing NRL Problem.
	6. PERFORMING ORG. REPORT NUMBER
7. AUTHOR(s): Anthony E. Spezio	8. CONTRACT OR GRANT NUMBER(s)
9. PERFORMING ORGANIZATION NAME AND ADDRESS: Naval Research Laboratory, Washington, D.C. 20375	10. PROGRAM ELEMENT, PROJECT, TASK AREA & WORK UNIT NUMBERS: NRL Problem R06-73; 36GG; NAVELEX 320
11. CONTROLLING OFFICE NAME AND ADDRESS: Naval Electronic Systems Command, Washington, D.C. 20360	12. REPORT DATE: December 28, 1978
	13. NUMBER OF PAGES: 40
14. MONITORING AGENCY NAME & ADDRESS *(if different from Controlling Office)*	15. SECURITY CLASS. *(of this report)*: UNCLASSIFIED
	15a. DECLASSIFICATION/DOWNGRADING SCHEDULE

16. DISTRIBUTION STATEMENT *(of this Report)*

Approved for public release; distribution unlimited.

17. DISTRIBUTION STATEMENT *(of the abstract entered in Block 20, if different from Report)*

18. SUPPLEMENTARY NOTES

19. KEY WORDS *(Continue on reverse side if necessary and identify by block number)*

Ionized meteor trails
Meteor-burst communication link
Radio-wave propagation

20. ABSTRACT *(Continue on reverse side if necessary and identify by block number)*

Radio-wave propagation via scattering from ionized meteor trails has been studied and employed as a means of communications for several decades. From the empirical and analytical data acquired, a propagation model to be used for communication link design can be extracted. This document derives and presents such a propagation model.

Empirical data were obtained from the observation of meteor trail occurrences and intensities. The propagation model was developed as a function of the pertinent parameters by examining the

(Continues)

DD FORM 1 JAN 73 1473 EDITION OF 1 NOV 65 IS OBSOLETE
S/N 0102-014-6601

SECURITY CLASSIFICATION OF THIS PAGE *(When Data Entered)*

20. Abstract (Continued)

transmission equation, the empirical data, and the geometric considerations. In this way, the characteristics of the meteor trail communication link were reduced to a manageable number of single and dual independent parameter equations and graphs that are suitable for system design and analysis. Examples were provided for utilizing the design equations in analyzing and synthesizing the meteor-burst communication link.

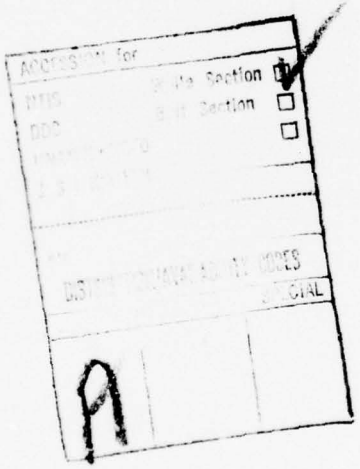

CONTENTS

METEOR PROPAGATION COMMUNICATION LINK DESIGN CONSIDERATIONS

INTRODUCTION

The purpose of this report is to establish a quantitative appreciation for the mechanics associated with providing a communications link effected via meteor scatter and reflection. A major portion of this report is devoted to the discussion of the propagation and statistical characteristics associated with the meteor ionization trails. The results of this discussion will then be applied to communications systems to determine hardware parameters required to effect the desired link.

METEOR INCIDENCE PHENOMENON

The earth's atmosphere accumulates a large number of meteor particles each day, and these particles are subject to random variations as well as predictable diurnal and seasonal variations.

Table 1 suggests that sizes of meteors range from those with a mass of 10 kg and a radius of 8 cm to those with a mass of 10^{-12} g and a radius of fractions of a micrometer. The number of incident meteors, however, is inversely proportional to the mass, ranging from an occurrence rate of 10 per day for meteors in the 10-kg range to 10^{12} per day for meteors in the 10^{-7}-g range [1]. Of particular interest in generating a radio transmission path is the electron line density produced by these meteors, which is indicated in the far right-hand column of Table 1. The electron line density is shown to be directly proportional to mass, varying from 10^{18} electrons per meter for a 10-g meteor to 10^{10} electrons per meter for a 10^{-7}-g meteor.

The incidences of the meteors indicated in Table 1, subject to random, diurnal, and seasonal variations, are yearly averages. Figure 1, for example, shows the seasonal variations for meteor incidence at approximately 40°N latitude. The apparent meteor density is six times greater in the summer and fall months than in the winter and spring. This is because of the seasonal tilt of the northern hemisphere away from the earth's direction of travel in the summer and early fall months. The ratio of seasonal variations in the meteor occurrence rate is 6 . It should be noted that these variations tend to be maximum at the poles and minimu at the equator. As one would expect, the seasonal variations in the southern hemisphere are just the opposite of those experienced in the northern hemisphere.

In addition to the seasonal variations, diurnal variations also have a strong influence on the incidence of meteor bursts. These variations result from the earth's traveling through

Manuscript submitted April 6, 1978.

Table 1 — Order-of-Magnitude Estimates of the Properties of Sporadic Meteors [1]

Meteor Particles	Mass (g)	Radius	Number of This Mass or Greater Swept Up by the Earth Each Day	Electron Line Density (electrons per meter of trail length)
Particles pass through the atmosphere and fall to the ground	10^{4}	8 cm	10	—
Particles totally disintegrated in the upper atmosphere	10^{3}	4 cm	10^{2}	—
	10^{2}	2 cm	10^{3}	—
	10	0.8 cm	10^{4}	10^{18}
	1	0.4 cm	10^{5}	10^{17}
	10^{-1}	0.2 cm	10^{6}	10^{16}
	10^{-2}	0.08 cm	10^{7}	10^{15}
	10^{-3}	0.04 cm	10^{8}	10^{14}
	10^{-4}	0.02 cm	10^{9}	10^{13}
	10^{-5}	80 μm	10^{10}	10^{12}
Approximate limit of radar measurements	10^{-6}	40 μm	10^{11}	10^{11}
	10^{-7}	20 μm	10^{12}	10^{10}
	10^{-8}	8 μm	?	?
Micrometeorities (Particles float down unchanged by atmospheric collisions)	10^{-9}	4 μm	Total for this group estimated as high as 10^{20}	Practically none
	10^{-10}	2 μm		
	10^{-11}	0.8 μm		
	10^{-12}	0.4 μm		
Particles removed from the solar system by radiation pressure	10^{-13}	0.2 μm	—	—
	—	—	—	—

space in the direction of the dawn semicircle. The portion of the earth traveling at the greatest forward speed with the maximum forward surface area is that portion of earth experiencing dawn. This diurnal effect on the occurrence of meteor trails is shown in Fig. 2. We can see that the number of trails increases as the time approaches 0600, decreasing very rapidly thereafter, and that the diurnal variation is 4:1. Diurnal variations, contrary to seasonal variations, show maximum excursions at the equator and much smaller variations at the poles.

The seasonal and diurnal variations associated with the occurrence of a meteor trail propagation path can quite easily produce an overall variation of 24:1 on the mean probability of communication path occurrences over a one-year period. Therefore, in the design of a communication system using meteor trails, these variations must be taken into consideration.

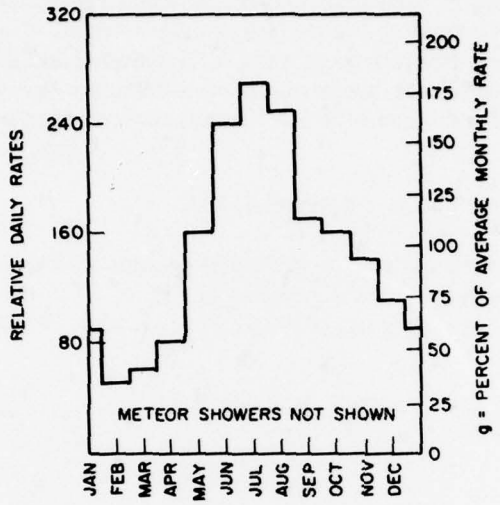

Fig. 1 — Seasonal variation of sporadic meteor rates including values for "g" in percent

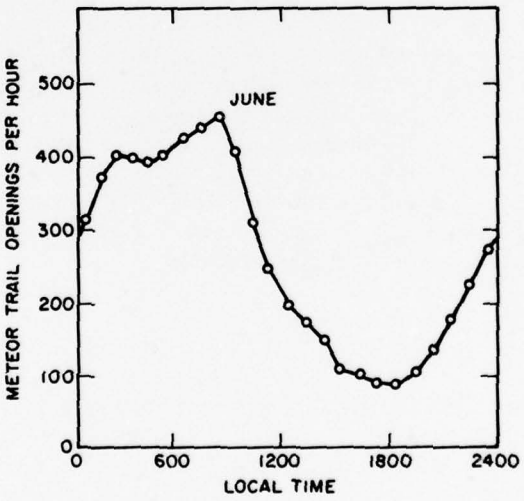

Fig. 2 — Relative average diurnal meteor trail rates

Consider a link requirement of N channel openings per hour in which the link is designed to have a mean of N channel openings. During some period of operation, there will be insufficient channel openings to provide the desired data transfer because of diurnal and seasonal variations. The link must be designed for a higher number of channel openings, to overcome this deficiency.

Due to the randomness of meteor incidence, channel openings will be probabilistic. To achieve a probability of attaining the desired number of channel openings in excess of 90 percent for a given hour requires provisions for a 10:1 seasonal and diurnal variation. Since the mean of an assumed worst-case, uniform-density variation is 5.5, the link with N channel openings per hour must be redesigned for 5.5 N mean channel openings per hour.

MECHANICS OF METEOR TRAIL PROPAGATION

The following paragraphs discuss the interrelationships among the various parameters of this communication system and the derivation of a group of design charts to facilitate analysis and system design involving meteor-burst propagation. The items that will be discussed include

Transmission equation
Channel duration
Channel openings
Antenna considerations
Date rate
Detectability.

Transmission Equation

A meteor passing into the earth's atmosphere produces a trail of ionized atoms having the density indicated in Table 1. To achieve a communication channel using this effect, we employ the trail of ions and free electrons as a scattering and/or reflecting medium. Trails with electron densities of 10^{14} electrons per meter or less produce a scattering of waves in the forward direction. These trails are termed *underdense*. Trails with electron densities greater than 10^{14} electrons per meter act as reflecting surfaces, producing a forward reflection of the wave off the meteor trail, and are termed *overdense*. The equations of propagation for each of these two conditions will be presented.

Underdense Condition

The transmission equation for the underdense condition is

$$\frac{P_R(t)}{P_T} = \frac{1}{32\pi^4}\left(\frac{\mu_0 e^2}{4m}\right)\frac{2\lambda^3}{R_1 R_2(R_1 + R_2)} \cdot \frac{G_R G_T q^2 \sin\alpha}{1 - \cos^2\beta \sin^2\phi} \exp\left(-\frac{32\pi^2 dt}{\lambda^2 \sec^2\phi}\right), \qquad (1)$$

where

P_R = received power

P_T = transmitter power

$\frac{\mu_0 e^2}{4m} = 0.8852 \times 10^{-14}$

μ_0 = permeability of free space

e = charge of an electron

m = mass of an electron

λ = wavelength

R_1, R_2 = ranges between the meteor trail and the transmitter and receiver

G_R, G_T = receiving and transmitting antenna gain

q = line density of electrons

α = angle between the electric vector of the incident wave and the path of the meteor

2ϕ = interior angle between the incident and scattered wave (the forward scattering angle)

β = angle between the axis of the meteor trail column and the plane containing transmission path

d = diffusion constant of the meteor column (8 m/s as established experimentally).

If the time variation of this function is ignored and if the minimum propagation loss is

$$\frac{P_R(0)}{P_T} = \frac{1}{32\pi^2}\left(\frac{\mu_0 e^2}{4m}\right)^2 \frac{2\lambda^3}{R_1 R_2 (R_1 + R_2)} \frac{G_R G_T q^2 \sin\alpha}{1 - \cos^2\beta \sin^2\phi}, \tag{2}$$

a number of simplifying assumptions can be made to reduce this equation [2].

First, $G_R G_T = 1$ antenna gain will be considered as isotropic. Effects of antenna gains will be considered later in this report.

Next, the trail is oriented to present a principal Fresnel zone. A trail gives a reflection only when incident and reflected rays meet the trail at right angles; i.e., $2\phi \approx 90^\circ$ (this assumption applies only to Eq. (2) where the value of ϕ is a second-order effect). Also, a random-direction incidence of meteors is assumed, resulting in a uniform distribution for the value of β and an average value of $\cos\beta = 2/\pi$. The transmission is assumed to be horizontally polarized: i.e., $\alpha = 90^\circ$.

Based on these assumptions, Eq. (2) reduces to

$$\frac{P_R(0)}{P_T} = \frac{1}{32\pi^4}\left(\frac{\mu_0 e^2}{4m}\right)^2 \frac{2\lambda^3}{R_1 R_2 (R_1 + R_2)} \frac{q^2}{1 - \left(\frac{2}{\pi}\right)^2 \left(\frac{1}{\sigma^2}\right)^2}. \tag{3}$$

Let $\lambda = c/f$, where f = transmission frequency. Then

$$\frac{P_R(0)}{P_T} = \frac{1}{16\pi^4}\left(\frac{\mu_0 e^2}{4m}\right)^2 \frac{C^3}{1 - \frac{2}{\pi^2}} \frac{q^2}{R_1 R_2 (R_1 + R_2) f^3}. \tag{4}$$

In Eq. (4), the expression

$$\frac{1}{16\pi^4}\left(\frac{\mu_0 e^2}{4m}\right)^2 \frac{C^3}{1 - \frac{2}{\pi^2}}$$

is a constant equal to 17.024×10^{-7}.

Hence, Eq. (4) becomes

$$\frac{P_R(0)}{P_T} = 17.024 \times 10^{-7}\left(\frac{q^2}{R_1 R_2 (R_1 + R_2) f^3}\right). \tag{5}$$

As seen in Eq. (5) for the underdense condition, the path loss (assuming $R_1 \approx R_2$) is inversely proportional to the square of the electron density and directly proportional to the third power of the operating frequency and the third power of the station-to-meteor distance. A plot of Eq. (5) is shown in Fig. 3 for $R_2 = R_1 = 510$ km, $f = 30$ MHz, and q ranging from 10^{10} to 10^{14} electrons per meter. The path loss for these conditions varies from 255 dB at $q = 10^{10}$ to 175 dB at $q = 10^{14}$. These losses can be compared with the 125-dB loss incurred in line-of sight propagation.

Overdense Condition

The transmission equation for the overdense condition is [2]

$$\frac{P_R(t)}{P_T} =$$

$$\frac{G_T G_R}{32\pi^4}\left(\frac{\mu_0 e^2}{4m}\right)^{1/2}\frac{\lambda^3 \sin^2\alpha q^{1/2}}{R_1 R_2 (R_1+R_2)(1-\cos^2\beta\sin^2\phi)}\left[dt\,\ell n\left(\frac{\mu_0 e^2 q\lambda^2 \sec^2\phi}{16m\pi^3 dt}\right)\right]^{1/2}. \quad (6a)$$

Since

$$dt\,\ell n\left(\frac{\gamma_0 e^2 q\lambda^2\,\sec^2\phi}{16m\pi^3 dt}\right), \quad (6b)$$

Eq. (6b) is the time-varying transmission equation factor, finding its maximum point defines the minimum transmission loss. To derive this maximum, first substitute

$$\tau = \frac{\gamma_0 e^2 q\lambda^2 \sec^2\phi}{16m\pi^3}$$

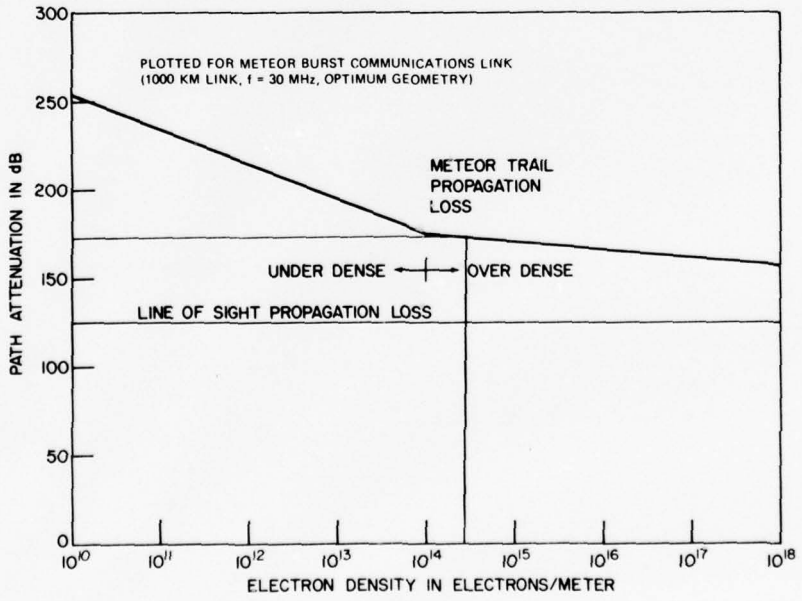

Fig. 3 — Electron density vs path attenuation (1000-km link, f = 30 MHz)

and

$$x = dt.$$

The time-varying factor then becomes

$$x \ln\left(\frac{\tau}{x}\right) = x[\ln(\tau) - \ln(x)] = \ln(\tau) - x \ln(x).$$

The minimum point of this function can be found by setting its derivative equal to zero:

$$x \cdot 0 + \ln\tau - x\left(\frac{1}{x}\right) - \ln(x) = \ln(\tau) - \ln(x) - 1 = 0$$

or

$$\ln\left(\frac{1}{x}\right) = 1.$$

Solving for x yields

$$x = \frac{\tau}{\epsilon},$$

where ϵ is the natural logarithm base. Substituting into Eq. (6b) yields

$$x \ln\left(\frac{\tau}{x}\right) = \frac{\tau}{\epsilon} x \ln\left(\frac{\tau}{\tau/\epsilon}\right) = \frac{\tau}{\epsilon} \ln\epsilon = \frac{\tau}{\epsilon}.$$

Substitute τ/ϵ into Eq. (6) to derive the minimum transmission loss during the overdense meteor-burst condition:

$$\frac{P_{R(\tau/\epsilon)}}{P_T} = \frac{R_T G_R}{32\pi^4}\left(\frac{\mu_0 e^2}{4m}\right)^{1/2}\left(\frac{\tau}{\epsilon}\right)^{1/2} \frac{\lambda^3 \sin^2\alpha q^{1/2}}{R_1 R_2 (R_1 + R_2)(1 - \cos^2\beta\sin^2\phi)}, \quad (7)$$

where $\tau = (16m\pi^3 d/\mu_0 e^2 q\lambda^2 \sec^2\phi)$. With the same simplifying assumptions applied to Eq. (2), it may be expressed in the form

$$\frac{P_R(\tau/\epsilon)}{P_T} = \frac{1}{32\pi^4}\left(\frac{\mu_0 e^2}{4m}\right)^{1/2}\left(\frac{\tau}{\epsilon}\right)^{1/2}\frac{1}{1-2/\pi^2}\frac{\lambda^3 q^{1/2}}{R_1R_2(R_1+R_2)}\,. \tag{8}$$

Let $\lambda = c/f$. Then,

Let

$$\frac{P_R(\tau/\epsilon)}{P_T} = \frac{1}{32\pi^4}\left(\frac{\mu_0 e^2}{4m}\right)^{1/2}\left(\frac{\tau}{\epsilon}\right)^{1/2}\frac{C^3}{1-2/\pi^2}\frac{q^{1/2}}{R_1R_2(R_1+R_3)f^3}\,. \tag{9}$$

In Eq. (9),

$$\left[\frac{1}{32\pi^4}\left(\frac{\mu_0 e^2}{4m}\right)^{1/2}\left(\frac{\tau}{\epsilon}\right)^{1/2}\frac{C^3}{1-(2/\pi)^2(.707)^2}\right]$$

is a constant equal to 12.7×10^{14}.

Equation (9) then becomes

$$\frac{P_R(\pi/\epsilon)}{P_T} = 12.7\times 10^{14}\left(\frac{q^{1/2}}{R_1R_2(R_1+R_2)f^3}\right). \tag{10a}$$

Here again, the transmission equation is reduced to a function of the same three variables found in Eq. (5) for the underdense case. In the overdense condition, the path loss is inversely proportional to the square root of the electron density and directly proportional to the third power of the operating frequency and the third power of the station-to-meteor distance.

A plot of Eq. (10) is shown in Fig. 3 for $R_2 = R_1 = 510$ km, $f = 30$ MHz, and q ranging from 10^{14} to 10^{18} electrons per meter. The path loss for these conditions varies from 175 dB at $q = 10^{14}$ to 155 dB with $q = 10^{18}$. Also, Fig. 3 shows the optimum transmission loss for a 1000-km link as a function of q. It should be noted that for the underdense condition the path loss varies as $1/q^2$, whereas for the overdense condition this loss varies as $1/q^{1/2}$ (i.e., in the underdense condition the loss decreases 20 dB for each order-of-magnitude increase in the electron density q, and in the overdense condition the loss decreases only 5 dB for each order-of-magnitude increase in the electron density q. Equations (5) and (10a), it will be noted, exhibit identical functional relationships with respect to frequency and geometry. These relationships of frequency and geometry to path loss can then be considered identical regardless of whether we are considering the overdense or underdense case.

The path loss of Fig. 3 may then be modified at a given frequency f by adding or subtracting the loss as indicated in the expression,

$$L_1 = 30 \log_{10} (f/30) \text{ dB}, \tag{10b}$$

where f = frequency in megahertz. This equation is applicable for the range of 10 to 100 MHz, limited at low frequency by the apparent meteor trail length and at high frequency by the excessive loss incurred.

The path loss of Fig. 3 may also be modified for other station separations, as shown in the optimum-geometry plot of Fig. 4. For the optimum geometry (minimum path length),

$$R_1 = R_2 = (100^2 + (\frac{D}{2})^2 \text{ km}, \tag{11}$$

where D = station separation in kilometers and the altitude of the meteor burst is 100 km. The path loss of Fig. 3 may then be modified at a given station separation D by adding or subtracting the loss indicated in

$$L_2 = 30 \log_{10} (R/510) \text{ dB}, \tag{12}$$

where R is obtained from Eq. (11).

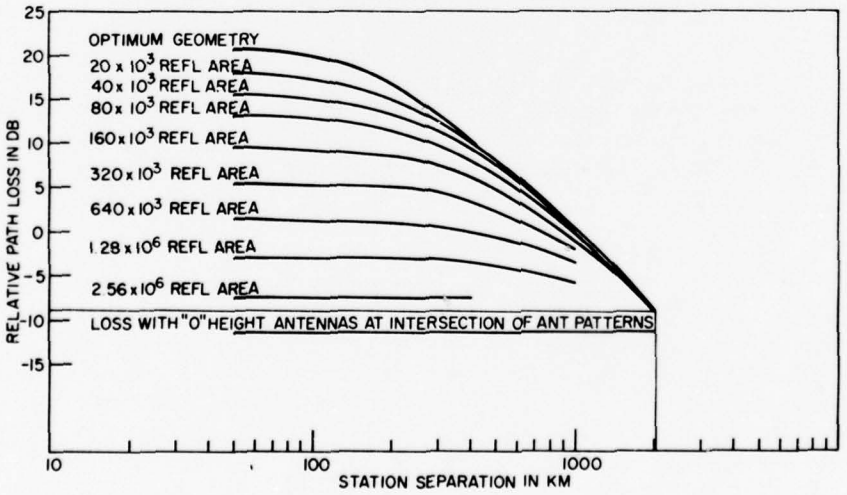

Fig. 4 — Reflection path loss vs station separation

Application of this equation to various station separations yields the optimum geometry curve of Fig. 4. This plot indicates that (with the value obtained for the 1000-km station separation as a reference) the loss increases from approximately 20 dB less than the reference value for a station separation of 50 km to a loss approximately 10 dB greater than the reference value for a station separation of 2000 km. It is noted that at the smaller station separations (50 to 200 km), the loss remains nearly constant, since the path under consideration is mostly vertical. Beyond this point, however, the loss becomes proportional to the third power of the station separation, as one would expect.

The area of overlapping antenna coverage must be considered in the design of this system. This overlapping coverage is termed the *reflection area.* All meteors of sufficient strength and proper orientation in this area will produce a channel opening. For purposes of simplification, the reflection area will be defined here as the largest circle contained in the area of overlapping coverage.

The relative path loss associated with an area of antenna coverage may be determined by establishing the desired area of coverage A as shown in Fig. 5. Since the assumption is made that the area of coverage is circular, then

$$r = (A/\pi)^{1/2}, \tag{13}$$

where r = radius of A. The maximum propagation path length is given as

$$R_1 = R_2 = (100^2 + (\frac{D}{2})^2 + r^2)^{1/2}. \tag{14}$$

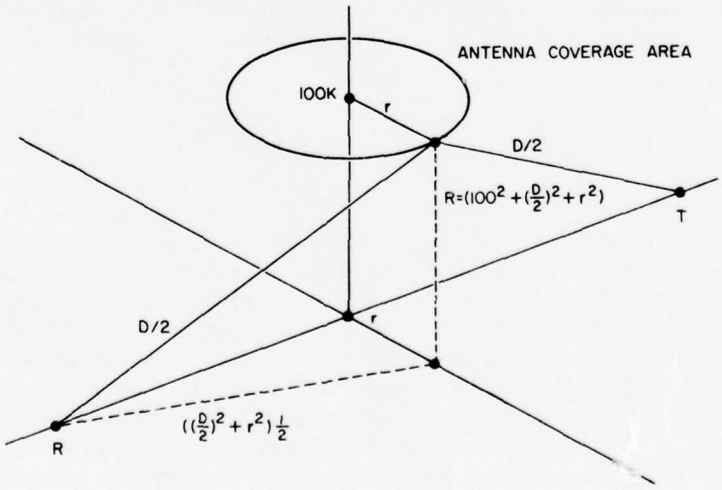

Fig. 5 — Maximum path length for meteor-burst geometry

The results of this equation may then be applied to Eq. (12) to obtain the relative path loss associated with a given area of coverage. Figure 4 shows a number of relative insertion losses plotted for various reflection areas as a function of station separation. These losses tend to converge to the relative value for optimum geometry as the station separation increases. This relationship occurs when D becomes larger than r in the square root of the sum of the squares (Eq. (14)). This figure also indicates that limiting the reflecting area at lower station separations reduces the overall path loss of the link.

Channel Duration

The previous paragraph deferred consideration of the time-related properties of the transmission path. They are considered here since it is of great importance to know the duration of the channel opening and the time-varying amplitude characteristics of this opening. From Eq. (1), we take the time-varying relationship for the underdense condition as

$$J_1 = \exp\left(-\frac{32\pi^2 d\epsilon}{\lambda^2 \sec^2\phi}\right), \tag{15}$$

which describes an exponential decay with a time constant of

$$\tau = \frac{\lambda^2 \sec^2\phi}{32\pi^2 d} . \tag{16}$$

Since the denominator of Eq. (16) is a constant, the time constant is a function of frequency and the forward scattering angle only. In this case, τ is heavily dependent upon ϕ; this term cannot be neglected. This equation may be evaluated for a spherical earth at various ranges D if we let

$$\sec\phi = R/\left[100 + 6400 - \sqrt{(6400)^2 - (0.5D)^2}\right],$$

where 100 km is the meteor-burst ionization altitude, 6400 km is the earth's radius, D = the distance between stations, and R = propagation distance, as determined in Eq. (14). Figure 6 is obtained by evaluating this expression for λ = 10 m (30 MHz) and for various reflection areas. The link time constant for various reflection areas at various station separations is given. This curve shows a significant propagation time constant increase as station separation lengthens (as ϕ becomes larger). For a 20,000-km^2 reflection area, the time constant increases from 40 ms at a 50-km station separation to 1.2 s at a 2000-km station separation. This explains the relative success of links established with station separations between 800 km and 1500 km. This curve also indicates that for increasing areas of coverage there will be a decrease in the time constant of the channel.

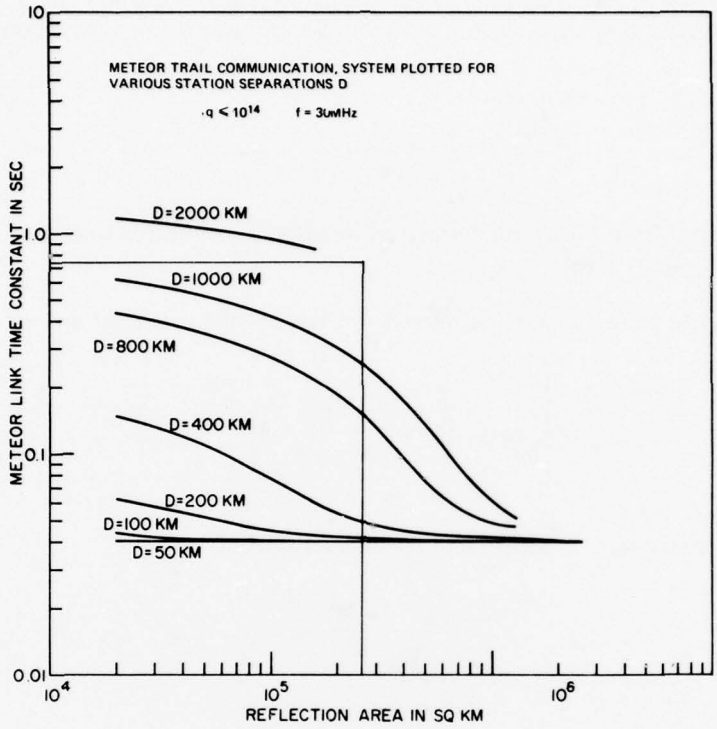

Fig. 6 — Meteor-link time constant vs reflection area

From Eq. (16), it is apparent that the time constant is also a function of frequency. To account for this variable relative to the results of Fig. 6, we scale this result by the factor

$$\tau = (30/f)^2. \tag{17}$$

This function indicates a decreasing time constant with increasing frequency. With Fig. 6 and Eq. (17), the propagation time constant may be determined.

The function of the time constant generated above must now be investigated to determine its effect on the propagation loss for a transmission of a desired duration. Since Eq. (15) demonstrates that the time-varying portion of the transmission equation is an exponentially decaying function, use of the channel for any period of time during the meteor burst requires that the characteristics of this function be taken into account. The amplitude function of the decay varies according to the function

$$L_3 = 10 \log_{10} e^{-t/\tau} \text{ dB}. \tag{18a}$$

This function is plotted in Fig. 7 where $q < 10^{14}$. This establishes the additional path loss to be applied to the system when a time T is desired for transmission. A time-constant factor,

$$K = T/\tau, \tag{18}$$

may be computed and, from Fig. 7, an additional loss may be obtained that must be compensated for in the system design.

From Eq. (7), the time-varying relationship for the overdense condition is

$$J_2 = \left[td\, \ell n \left(\frac{\mu_0 e^2 q \lambda^2 \sec^2 \phi}{16 m \pi^3 td} \right) \right]^{1/2}, \tag{19}$$

which describes a logarithmic response with a time constant of

$$\tau' = \frac{\mu_0 e^2 q \lambda^2 \sec^2 \phi}{16 m \pi^3 d}. \tag{20}$$

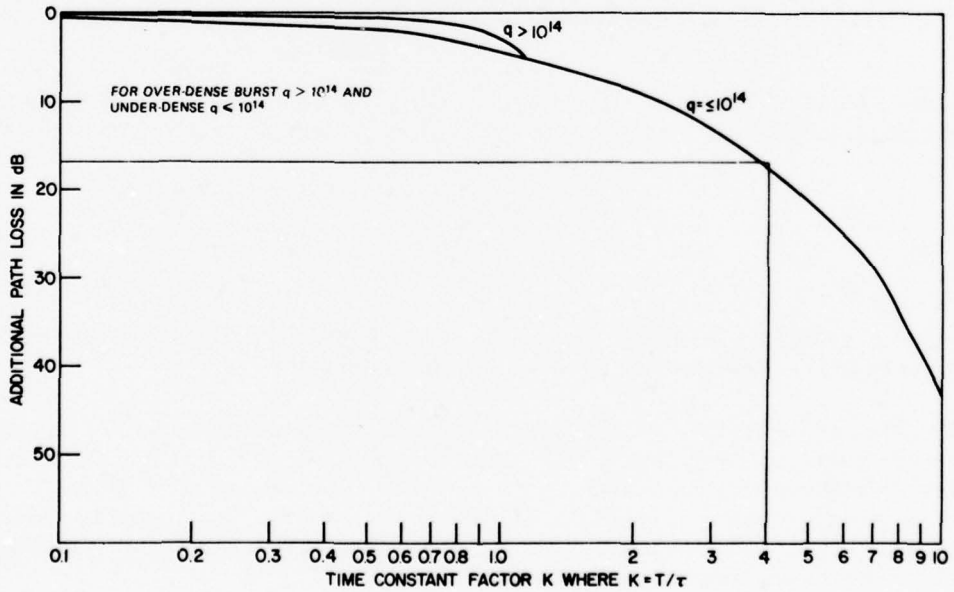

Fig. 7 — Additional path loss vs time-constant factor K

Since $\mu_0 e^2/16m\pi^3 d$ is a constant, the overdense time constant is a function of frequency λ, forward scattering angle ϕ, and electron line density q. Note that the functional relationships among the time constant, frequency, and scattering angle are identical for the overdense and underdense conditions. The underdense condition time constant has no functional relationship to the electron line density. It is further observed that $\tau = \tau'$ (Eq. (16) = Eq. (20) for $q \cong 0.75 \times 10^{14}$). Therefore, it follows that because of identical frequency and forward-scattering-angle relationships between underdense and overdense time constants and, because of equality of these two functions for $q \approx 10^{14}$, the results of Fig. 6 are applicable to the overdense time constant directly at $q = 10^{14}$ and can be applied for $q > 10^{14}$.

Define

$$Q = q/10^{14}; \tag{21}$$

then

$$\tau' = Q\tau. \tag{22}$$

Equation (19) dictates that the time-varying portion of the overdense transmission equation is a logarithmically dependent function. A computation of the time-varying amplitude function was made by evaluating the equation

$$L4 = 5 \log_{10} [8\, t\ell n(\tau'/t)]. \tag{23}$$

The results of the evaluation of this function are shown as the $q > 10^{14}$ curve in Fig. 7. The conclusion of these results is that an overdense propagation path exhibits less amplitude decay over the first time constant than does an underdense path.

Channel Openings

With the propagation characteristics of a meteor trail defined, the next task at hand is to determine the number of trails available for use. Additional simplifying assumptions must be postulated concerning the geometric and statistical nature of the problem.

Assumptions

1. All meteor trails have the same length, 25 km, as determined experimentally.

2. Ionization occurs at 93 km above the earth's surface, as determined experimentally.

3. Only trails that are contained in a plane normal to the bisector of the forward-scattering angle will produce a return.

4. The meteors considered in this model are uniformly distributed over the earth.

5. The angles of incidence of the meteors are also random and uniformly distributed.

With these assumptions, a probability density function was generated that predicts the percentage of usable meteor trails per unit area that can be expected. This equation is

$$P = \frac{2\ell[3(E^2-N^2)-(1-N^2)][E^2-1)(E^2-N^2)-E^2H^2/(5D)^2] - N^2(E^2-1)H^2/5D^2}{1.5D(E^2-N^2)^2(E^2-1)[E^2-1)(E^2-N^2)-E^2H^2/(0.5D)^2]^{1/4}} \tag{24}$$

where

$E = (R_1 + R_2)/D$

$N = (R_1 - R_2)/D$

R_1, R_2 as defined in Eq. (14)

ℓ = meteor trail length, 25 km

H = altitude of meteor trail occurrence, 93 km.

Note from Eq. (24) that the probability density is a function of the path lengths R_1 and R_2 and the station separation D. As shown in Eqs. (13) and (14), R_1 and R_2 are functions of reflection areas as well as of station separation. The total number of channel openings C in a given area may be determined by evaluating the equation

$$C = A\iint P\, dR_1\, dR_2. \tag{25}$$

This equation was evaluated for discrete increments of reflection areas at several station separations. This evaluation resulted in Fig. 8, which shows the expected number of channel openings per hour as a function of the reflection area where $q = 10^{14}$. In Fig. 8, channel openings increase as reflection area increases. The increase in channel openings, however, is less than directly proportional to the reflection area. This degradation is more pronounced for smaller station separations and becomes almost directly proportional at station separations of 800 km or more.

Table 1 shows that the relationship between electron line density and rate of meteor occurrence is one of inverse proportionality. Because of this relationship, Fig. 8 may be used to establish the average electron line density to be used for propagation. To accomplish this, determine the ratio of the number of channel openings available for a given link distance and reflection area to the number of channel openings desired, and scale accordingly;

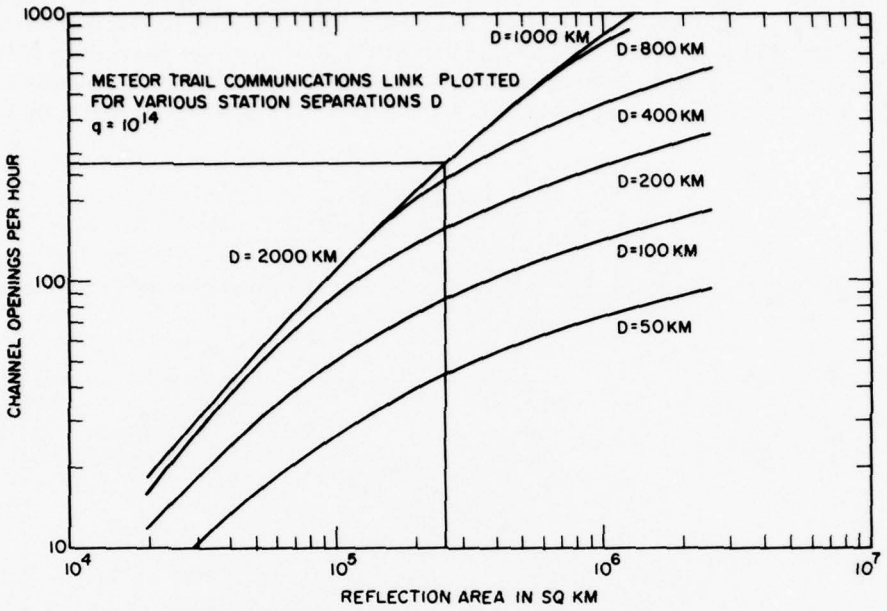

Fig. 8 — Channel openings per hour vs reflection area

$$q = \frac{\text{channel openings available} \mid A,D}{\text{channel openings desired}} \times 10^{14}. \tag{26}$$

With the value of q established from Eq. (26), the basic link loss may be obtained from Fig. 3.

Antenna Considerations

Designing an antenna for a meteoric propagation system is complicated by the statistical and geometric considerations of meteoric path occurrences shown in Fig. 8 and the geometric relationship of path time constant shown in Fig. 6. In general, use of the antenna gain is advantageous in reducing the receiver-to-transmitter overall loss and is most beneficial when applied equally at both stations. In Eqs. (13) and (14) the radius r for the reflection area and the path length R were determined. From these quantities, we define the antenna beamwidth required to provide the reflection area coverage;

$$\theta = 2 \sin^{-1} (r/R), \tag{27}$$

where θ = antenna beamwidth. This equation was evaluated as a function of reflection area and station separation. The results of these computations are plotted in Fig. 9 where the classical results of plotting the antenna beamwidth vs area of coverage are shown. If it is desired to approach the reflection area from antenna physical contraints, it is possible to determine gain from the physical conditions, and, from gain, the antenna beamwidth, by using

$$\theta \approx (27{,}000/G)^{1/2}. \tag{28}$$

With θ calculated from Eq. (28), Fig. 9 may then be used to determine reflection area.

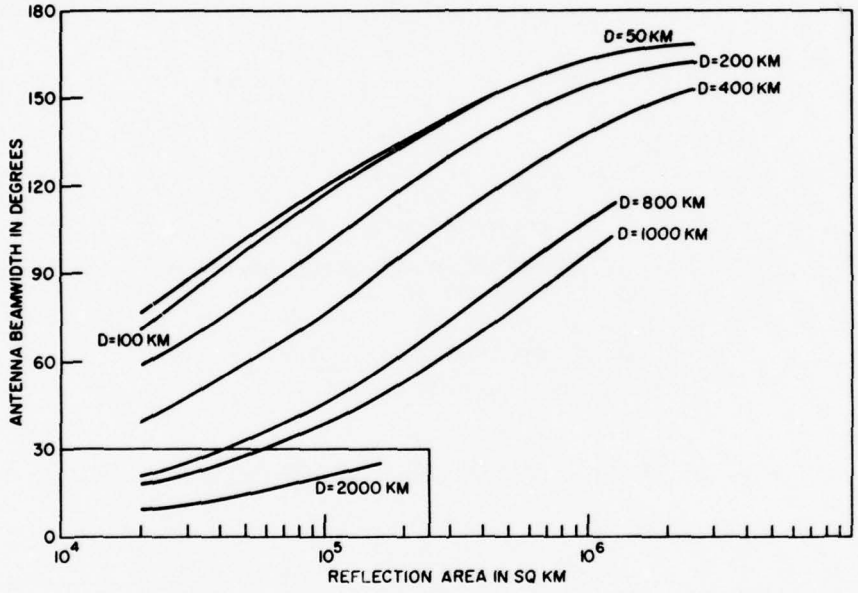

Fig. 9 — Antenna beamwidth vs reflection area

Data Rate

The mechanics affecting data rate and its limitations imposed by the physical phenomenon of meteor trail propagation have not been discussed in detail in the literature. To obtain an insight into some possible limitations of the system, we postulate that the point of reflection or scatter of the radio wave at the ionization column travels with the meteor as it travels through the atmosphere. It is further assumed that the predominance of meteors observed originate in the solar system, have an approximate orbit around the sun opposite to that of the earth's orbit, and, therefore, exhibit an average velocity with respect to the earth equal to twice the velocity of the earth with respect to the sun;

$$V_1 = 2\,\frac{\text{distance of earth travel/year}}{\text{seconds/year}}$$

$$V_1 = 2\,\frac{2\pi\ 93 \times 10^6 \times 1.6}{8{,}760\ \text{h/yr} \times 3600\ \text{s/h}} = 68.8\ \text{km/s}. \tag{29}$$

To determine the maximum time difference of arrival of a signal as the meteor traverses the atmosphere, assume that the meteor is incident to the earth's atmosphere in a plane normal to a line connecting the stations. The maximum range variations (km/s) may be computed from

$$\Delta R/\Delta t = 2[(0.5D)^2 + (100)^2]^{1/2} - [(0.5D)^2 + (100)^2 + (34.4)^2]^{1/2}. \tag{30}$$

From the results of this equation, the maximum difference of transmission time from the beginning of a transmission may be determined by us of

$$\frac{\Delta T}{\Delta t} = \frac{\Delta R/\Delta t}{3 \times 10^5\ \text{s/s}} \tag{31}$$

where $\Delta T/\Delta t$ is the propagation time change per unit of time. A certain amount of propagation time variation can be tolerated without causing appreciable intersymbol interference. The signal-to-noise degradation resulting from propagation time variations as a percentage of bit width is listed in Table 2.

Table 2—Multipath Signal Degradation

Time Delay/Bit Width (per bit)	S/N Degradation
0.1	1.0
0.2	2.2
0.3	4.0
0.4	7.0
0.45	10.0
0.49	20.0

Because the signal-to-noise ratio rapidly degrades as this ratio exceeds several tenths, it is necessary to restrict the data rate. Equation (31) was evaluated for various station separations and is illustrated in Fig. 10. The time delay decreases slowly for smaller station separations but decreases more rapidly as the station separation increases beyond 200 km. Figure 10 may be used to compute a maximum data-rate limit on a channel of interest, provided that the time duration τ of the transmission is established. This time is a function of the formatting requirements of the message and of the meteor time constant (see Fig. 6).

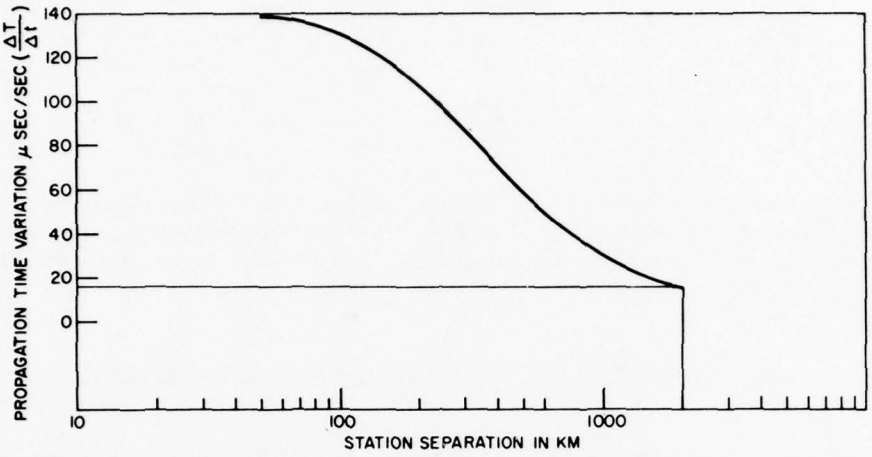

Fig. 10 — Propagation time variation vs station separation

Once time τ has been determined, the maximum data rate (using Fig. 10 and Table 2) can be computed as follows:

$$\text{Data rate} = \frac{\dfrac{\text{Time delay}}{\text{Bit width (dimensionless)}}\Big|_{\text{Fig. 10}}^{\text{Table 2}}}{\tau(\Delta T/\Delta\tau)} = \text{bits/s.} \tag{32}$$

For example, a 1000-km link D transmitting at 1-s intervals and incurring a 1-dB degradation due to time delay will have a maximum data rate of

$$\text{Data rate} = \frac{0.1}{1 \times 30.8 \times 10^{-6}} = 2.9 \text{ kbits/s.}$$

The time variation indicated by Eq. (31) is also capable of producing a doppler shift in the frequency at the receiver. This doppler shift must be accounted for by providing additional predetection bandwidth in the receiver. This increase in bandwidth required to operate the link in this case is given by the equation

$$\Delta F_{max} = 2f\frac{\Delta T}{\Delta t}, \tag{33}$$

where ΔF (doppler frequency) is the increase in bandwidth required to compensate for doppler. The increased bandwidth will also produce an increase in receiver noise by increasing the bandwidth factor of kTB.

Data-rate limitations, defined by Eq. (32), and sensitivity degradations corresponding to bandwidth increases (Eq. (33)) result in a simplified receiver configuration. However, the effects of this time variation and the associated degradation may be processed out of the system whenever the increased hardware complexity permits. For example, the bit rate may be substantially increased over that predicted in Eq. (32) by updating the bit synchronization at various times during the transmission. This can be accomplished by a "return to zero" format in the transmitted word structure and the associated hardware to update the bit synchronization, by applying the data to a pseudorandom code and using code synchronization, or by simply transmitting a fixed-format frame at a number of points in time during the transmission. The effects of doppler may be negated by incorporating an AFC loop in the associated receiver.

Detectability

The meteor-burst communication system has a number of advantages and disadvantages associated with undesired transmission interception. Of primary advantage is the random nature of the time occurrence of channel openings. Another advantageous characteristic of this system is the short duration of the transmission. Detection of signal strictly on a time basis is then a function of the number of channel openings and the time duration of the opening.

One of the detectability disadvantages is the additional power required to overcome the meteor reflection or scattering losses. Figure 3 indicates that power requirements in excess of line-of-sight requirements can vary from 25 to 125 dB for a nominal 1000-km meteor propagation link. The impact of this phenomenon is that even with a directive antenna to limit undesired radiation, a station is detectable at considerable line-of-sight ranges. To examine the magnitude of this problem, consider an example where the detection receiver has a −85 dBm sensitivity and a 1-MHz bandwidth, and the transmitting station applies 10 W of power into a 10-dB antenna with a forward-to-sidelobe ratio of 30 dB. Because of the 1-MHz bandwidth, this receiver has a high probability of acquiring the transmission, and the −85 dBm sensitivity permits a line-of-sight range to the transmitter of 400 km, with the received signal emanating from an antenna sidelobe.

The task of maintaining covert communications in a meteor propagation system can be seen to be quite formidable. A number of techniques may, however, be employed toward this end. Antenna sidelobe suppression and spread-spectrum transmission are among these.

SYSTEM ANALYSIS

This section is devoted to demonstrating the usefulness of the design aids derived heretofore. Two cases are considered for computational illustration. For these cases, experimental data have been obtained that afford a means of validating the analytical approach, and the link parameters for the analysis are extracted directly from the actual equipment. In the first case considered (the 900-km link), all system parameters except the transmitted power are obtained from the experimental data. The analytical tools of the previous section are used to determine the transmitted power. The experimental and computed transmitted power are then compared. In the second case (the 200-km link), all system parameters

except the channel openings per unit time are taken directly from the experimental data. This system is then analyzed to determine the number of channel openings per hour to be expected. And finally, the number of channel openings, determined analytically, is compared with the experimental results.

Analysis of a 900-km Link

A meteor propagation link covering 900 km is selected for analysis because of the availability of experimental data for this system. Comparison of the experimental transmitter power and the computed transmitter power indicates the relevance of the design relationships previously developed. The system parameters determined experimentally are

Receiver sensitivity		−115	dBm
Transmitter power		+ 50	dBm
Station separation		900	km
Receiver antenna gain	40	16	dB
Transmitter antenna gain	40	16	dB
Channel Openings		67/h	
Link duration		0.55	s
Frequency		50	MHz.

In this analysis, the transmitter power is assumed unknown and the analysis is directed toward a solution for this parameter. Initially, we are interested in determining the path loss between the two stations. Since Figs. 3, 4, and 7 show the path-loss functional dependence upon the electron line density q, the reflection area A, and the transmission time constant k, respectively, these parameters must be determined. The reflection area A (the overlap area) of the 3-dB beamwidth is employed. The antenna gain indicated in the system parameters is inserted into Eq. (28), which results in

antenna beamwidth $= \theta$,

and

$$\theta = \left(\frac{27{,}000}{G}\right)^{1/2} = \left(\frac{27{,}000}{40}\right)^{1/2} = 26^{\circ}.$$

With the antenna beamwidth determined and the station separation provided in the system parameters, the antenna pattern 3-dB overlap area A may be determined. Figure 9 presents the dependent relationship of reflection area A with respect to station separation D and antenna beamwidth 0. From this figure, we determine the reflection area by considering D = 900 km and $\theta = 26^{\circ}$:

From Fig. 9, beam overlap area = A
= reflection area = 37,000 km^2.

Once the overlap area A is determined, it is possible to obtain the required electron line density q. Thus, the number of channel openings available from a 37,000-km^2 overlap area at a standard electron line density of $q = 10^{14}$ is determined. Electron line density is inversely proportional to the desired channel openings, as indicated in Eq. (26). The available channel openings are determined from Fig. 8 and are entered into Eq. (26) to compute the required electron line density. Figure 8 gives the number of mean channel openings per hour to be expected for $q = 10^{14}$. Knowing antenna overlap area, A = 37,000 km^2, and the station separation, D = 900 km, we can find the number of channel openings available for $q = 10^{14}$:

A = 37,000 km^2, and $q = 10^{14}$,
channel openings per hour = 38

The actual value of electron line density required for this link is determined from Eq. (26) as a function of the ratio of the channel openings available to the channel openings desired, as given in the system parameters. From (26), electron line density = q, and

$$q = \frac{\text{Channel openings available}}{\text{Channel openings desired}} \times 10^{14}.$$

Thus,

$$q = \frac{38}{67} \times 10^{14} = 0.567 \times 10^{14}.$$

With A and q ascertained, it remains only to define K, the time-constant ratio that determines the path loss. The time-constant ratio K is the ratio of the desired transmission time to the link time constant τ, as shown in Eq. (18b). The link time constant τ, however, is a function of reflection area A, station separation D, and frequency f. Figure 6 illustrates link time constant as a function of reflection area and station separation for a frequency of 30 MHz. Equation (17) indicates the time-constant variation as a function of frequency. The link time constant is determined from Fig. 6 and Eq. (18b). The link time constant τ for the reflection area computed above, where A = 37,000 km^2 and D = 900 km (the station separation given in the system parameters) is 0.47 s.

The time constant derived from Fig. 6 must be modified to reflect the actual operating frequency f of 50 MHz as given in the system parameters. This is accomplished by evaluating Eq. (17).

From Eq. (17), link time constant = $\tau' = (30/f)^2\ (\tau) = (30/50)^2\ (0.47) = 0.169$ s
where f = operating frequency in megahertz.

With the link time constant computed and its value modified to reflect the desired operating frequency f, the time constant factor, defined by Eq. (18b) as the ratio of the transmission time given in the system parameters to the link time constant, is

$$k = \frac{\text{Transmission time}}{\tau'} = \frac{0.55}{0.169} = 3.25.$$

At this point, we have determined the variables having a functional relationship to the path loss. The next step in the process of computing required transmitter power is to calculate the path loss associated with the transmission media. This loss is a function of five variables: electron line density q, reflection area A, time constant factor K, frequency f, and station separation D. The path losses associated with each of these variables are calculated as follows:

First, the loss for an equivalent 1000-km link operating at 30 MHz with $q = 0.567 \times 10^{14}$ is determined from Fig. 3 to be..... 180 dB.

Then, this loss must be scaled by the actual frequency of operation. From Eq. (10b), $L_1 = 30 \log (f/30) = 30 \log 50/30 =$.....6.7 dB.

Figure 4 permits additional scaling to the antenna coverage area and the station separation distance; when A = 37,000 sq km and D = 900 km, then Δloss = ...—1.0 dB.

Due to the transmission time required in an exponentially decaying channel, the additional time-constant loss must be overcome. When K = 3.25 (time constant factor Eq. (18b), the time-constant loss (Fig. 7) =.....13.0 dB.

These losses are summed to present the overall path loss to be overcome in the channel .....198.7 dB.

With the path loss calculated, the transmitter power required to effect the link may be determined through use of conventional communication system analysis techniques. The transmitter power required can be found by working back from the receiver to the transmitter. The field strength in dBm required at the receiver is determined by subtracting the receiver antenna gain in decibels from the receiver sensitivity in dBm (both given in the system parameters). Thus,

Sensitivity	115 dBm
Receiver antenna gain	16 dB
Receiver field strength	−131 dBm.

With the receiver field strength and the total path loss computed, the transmitter effective radiated power (ERP) may be determined. To this end, the receiver field strength is added to the total path loss:

Receiver field strength	−131.0 dBm
Total path loss	198.7 dB
Transmitter ERP	67.7 dBm.

To determine the actual transmitter power required, we need only to subtract the transmitter antenna gain from the transmitter:

Transmitter ERP	67.7 dBm
Transmitter antenna gain	16 dB
Transmitter power	51.7 dB.

Performing this operation yields a 51.7-dBm transmitter power requirement that agrees favorably with the experimental results, indicating a required transmitter power of 50 dbM. The close agreement between the transmitter powers determined analytically and experimentally illustrates the applicability of the relationships of the procedures developed to the actual meter propagation problems.

Analysis of a 200-km Link

Additional assurance of the applicability of the mechanics developed will now be shown by analyzing a significantly different communication link capable of communication over a 200-km link. In this analysis system, parameters (with the exception of channel opening rate) are extracted directly from the experimental data and are used in conjunction with the logic developed to derive the channel opening rate. The system parameters determined experimentally are

Receiver sensitivity		−115 dBm
Transmitter power		+ 53 dBm
Station separation		200 km
Receiver antenna gain	20	13 dB
Transmitter antenna gain	20	13 dB
Channel openings		81/h
Link duration		0.05 s
Frequency		50 MHz.

In this analysis, the number of channel openings is assumed unknown and the analysis is directed toward a solution for this parameter. The approach to the solution for this system configuration is somewhat similar to the approach taken in the precing example. In this example, the total path loss is computed from the experimental data. With the total path loss determined, the number of channel openings of the desired length is then determined. To determine the path loss, first compute the field strength required at both the receiver and transmitter and then calculate the difference. The field strength in dBm required at the receiver is determined by subtracting the receiver antenna gain in divibils from the receiver sensitivity in dBm (both are given in the system parameters):

Sensitivity	−115 dBm
Receiver antenna gain	13 dB
Field strength at receiver	−128 dBm.

Conversely, the field strength in dBm available at the transmitter (ERP) may be determined by adding the transmitter antenna gain in decibels to the transmitter power in dBm:

Transmitter power	53 dBm
Transmitter antenna gain	13 dB
Transmitter ERP	+66 dBm.

With the field strengths computed for both the receiver and transmitter, finding the allowable path loss becomes simply a matter of subtracting those two numbers.

Transmitter ERP	+ 66 dBm
Field strength at receiver	−128 dBm
Total path loss	194 dBm.

Once the total path loss is known, the individual contributions to this total loss may be calculated. As indicated in the previous example, Figs. 3, 4, and 7 depict path loss as showing functional dependence on electron line density q, reflection area A and the transmission time constant ratio K, respectively. The initial task then becomes one of determining these values. The reflection area A, i.e., the overlap area of the 3-dB beamwidth of the transmitting and receiving antennas at the meteor trail altitude of 100 km, is determined. Equation (28), relating antenna beamwidth to antenna gain, is used to compute the antenna beamwidth. The antenna gain given in the system parameters is substituted in Eq. (28) to provide the antenna beamwidth. From Eq. (28),

antenna beam width,

$$\theta = \left(\frac{27{,}000}{G}\right)^{1/2} = \left(\frac{27{,}000}{20}\right)^{1/2} = 47^{\circ}.$$

From the antenna beamwidth computed above and with the station separation given, the reflection area A may be determined. The relationship of reflection area A to station separation D and antenna beamwidth θ is shown in Fig. 9. From this figure, the reflection area is determined by identifying this area with respect to a station separation of 200 km and an antenna beamwidth of 47°. For D = 200 km and $\theta = 47^{\circ}$, A = 12,000 sq km.

As shown by Eq. (18b), the time constant factor K is the ratio of the desired transmission time to the link time constant τ. The link time constant τ, however, is a function of reflection area A, station separation D, and operating frequency f. See Fig. 6. Equation (17), in conjunction with Fig. 6, provides the link time constant, and Eq. (18b) is used to ascertain the time constant factor K. The link time constant for a reflection area of 12,000 km^2, station separation of 200 km, and frequency of 30 MHz is taken from Fig. 6 to be 0.07 s. This time constant must be modified to reflect the actual operating frequency f of 50 MHz. Evaluation of Eq. (17) gives

$$\tau' = \text{link time constant} = \left(\frac{30}{f}\right)^2 \tau = \left(\frac{30}{50}\right)^2 0.07 = 0.0252 \text{ s.}$$

This modified link time constant is now used in Eq. (18b) to compute the time constant factor,

$$K = \frac{\text{link duration}}{\tau'} = \frac{0.05}{0.0252} = 1.91.$$

In these computations, four of the five independent variables that constitute the argument of the total insertion loss were determined. It is now possible to solve for the path loss associated with the final independent variable q, and from this loss to determine q itself. Since channel openings are a direct function of q (electron line density), the number of channel openings may then be determined as the solution. The path losses associated with each of the four known variables (reflection area, time constant, frequency, and station separation) are calculated next. The results are combined and subtracted from the total path loss already determined.

A component of the path loss must be considered that accounts for the reflection area A covered by the overlapping antenna patterns and the station separation as differentiated from the standard 1000-km link. The loss variation ΔL considered with respect to these two parameters is plotted in Fig. 4 and is shown to be −16 dB for a reflection area of 12,000 km^2 and a station separation of 200 km.

An additional path loss considered here is the one associated with link duration. The path loss exponentially increases with the duration of the link. If an adequate system design for the entire transmission duration is to be provided, the link must be designed to operate at the end of the transmission period. The difference between the zero-time path loss and the end-of-transmission path loss is the time-constant loss, and is evaluated by entering Fig. 7 with the time constant computed above.

From Fig. 7, the time-constant loss for $K = 1.91 = 8.5$ dB.

The remaining loss to be computed is that associated with the operating frequency. Since all curves used were referenced to an operating frequency of 30 MHz, operating at a frequency of other than 30 MHz requires scaling the loss to the frequency of operation. The frequency given in the system parameters is used in Eq. (10b) to compute the frequency-associated loss.

$$\text{Loss} = L_1 = 30 \log(f/30) = 30 \log(50/30) = 6.7 \text{ dB}.$$

With the three loss factors and the total path loss determined, the loss associated with the electron line density q and, ultimately, the channel openings rate may be determined. To calculate this loss, we subtract the loss factors from the total path loss.

$$L = \text{total path loss} - L_1 - \Delta L - \text{time-constant loss}$$
$$L = 194 - 6.7 - (-16) - 8.5 = 194.8 \text{ dB}.$$

This optimum path loss can be related to the electron line density. Since this is the independent variable of the expression for the channel openings, its determination will be used as an intermediate step in computing the channel openings. Arriving at this value is accomplished by considering Fig. 3 at a loss of 194.8 dB and noting the corresponding electron line density q of 10^{13}.

Before the final number of channel openings available can be computed, it is necessary to determine the number of channel openings available at a standard electron line density $q = 10^{14}$. The base number of channel openings per hour is determined from Fig. 8 with antenna overlap area of 12,000 km^2 and station separation of 200 km. There are nine channel openings per hour for $q = 10^{14}$. The number of channel openings available for communication is a function of the actual electron density used in effecting a link. The nine channel openings computed are modified by applying this factor along with the actual electron line density used ($q = 10^{13}$) in Eq. (26).

$$q = \frac{\text{Channel openings available}}{\text{Channel openings desired}} \times 10^{14},$$

$$\text{Channel openings desired} = \frac{10^{14}\ \text{Channel openings available},}{q}$$

$$\text{Channel openings desired} = \frac{9 \times 10^{14}}{10^{13}} = 90 \text{ per hour.}$$

The figure of 90 channel openings predicted by the analytical results agrees very well with the 81 channel openings per hour determined experimentally.

SYSTEM DESIGN PROCEDURE

The mechanics thus far have been established as useful tools in describing the meteor-burst link. This section addresses the synthesis of a system employing meteor trail propagation. The requirements of system parameters are derived in this example.

Statement of the Problem

A system is desired that provides for data communication between an unattended weather buoy and a mainland station separated by a total distance of 1500 km. The buoy is required to reliably transmit 2000 bits of data an hour to the base station. Antenna stabilization cannot be employed and the buoy must operate unmoored. Additional hardware as required may be employed at the base station. In the interest of buoy longevity, consideration should be given to reducing its power requirements. The derivations of the parameters follow.

Derivation of Parameters

Buoy Antenna - An omnidirectional horizontally polarized antenna exhibiting as much antenna gain as practical is required for this parameter. For this application, an array consisting of a stacked pair of loaded loop antennas is used. This antenna provides approximately a 5-dB gain and a vertical beamwidth of 80°. The beamwidth is sufficient to provide communication even during substantial roll.

Base Station Antenna - Since fewer restrictions have been placed on the base station, an antenna loss chosen to compensate for gain not available at the buoy. The base station antenna selected is a rhombic that provides a 24-dB gain.

Frequency - Because of the increased losses incurred with increasing frequency, the lowest frequency consistent with physical limitations should be selected. For this example let us assume that this frequency is 35 MHz.

Reflection Area - The base station antenna design dictates that the reflection area A, i.e., the overlap area of the 3-dB beamwidth of the transmitting and receiving antenna at the meteor trail altitude of 100 km, will be determined. Equation (28), which relates antenna gain to antenna beamwidth to determine the antenna beamwidth, was employed. The gain indicated in the system parameters was inserted into this equation, the solution of which is the antenna beamwidth. Thus, antenna beamwidth,

$$\theta = \left(\frac{27{,}000}{G}\right)^{1/2} = \left(\frac{27{,}000}{251}\right)^{1/2} = 10.4°.$$

With the antenna beamwidth determined and the station separation provided in the system parameters, the antenna pattern 3-dB overlap area A may be determined. Figure 9 presents the dependent relationship of reflection area A with respect to station separation D and antenna beamwidth θ. When D = 1500 km and $\theta = 10.4°$, the reflection area is determined to be 15,000 km^2.

Data Rate - The channel data rate must be estimated in order to gain insight into the channel opening requirement. This is a function of the channel duration, so it is this parameter that must be determined initially. The link time constant τ, however, is a function of reflection area A, station separation D, and frequency f. Figure 6 determines link time constant as a function of reflection area and station separation for a frequency of 30 MHz. Equation (27) indicates that the time constant variation is a function of frequency. The link time constant is determined from Fig. 6 and Eq. (17), and the time constant ratio K is computed using Eq. (18b). The link time constant τ for the reflection area of 15,000 km^2 and the station separation given in the problem statement (1500 km) is determined from Fig. 6 to the 0.975. Since this is for a frequency of 30 MHz, this time constant must be modified to reflect the actual operating frequency f of 35 MHz. This is accomplished by evaluating Eq. (17). Thus,

$$\tau' = \left(\frac{30}{f}\right)^2 \tau = \left(\frac{30}{35}\right)^2 0.975 = 0.72 \text{ s}.$$

As a preliminary estimate to facilitate computation, the assumption is made that each transmission T will exist for two time constants, or 1.44 s. With the link time constant determined, it becomes possible to solve for the data rate using Eq. (32) as follows:

$$\text{Data rate} = \frac{\left(\frac{\text{Time delay}}{\text{Bit width}}\right)}{T\left(\frac{\Delta T}{\Delta \tau}\right)} \quad \begin{matrix}\text{(from Table 2)} \\ \text{(from Fig. 9)}\end{matrix}$$

The data rate is a multiple-variable function of two ratios: the ratio of channel time delay to bit width and that of the differential transmission time to the channel time constant. Hence, it is necessary to determine the values of these ratios before proceeding. The time-delay/bit-width ratio is the tolerable time instability compared to a bit duration in any part of a given message. Associated with this instability is a degradation in signal-to-noise ratio in the system. The degradation allowable is somewhat arbitrary initially and will be assumed to be 1 dB for this case. The ratio of time delay to bit width is determined from Table 2 at the 1-dB level.

$$\frac{\text{Time delay}}{\text{Bit width}} = 0.1 \text{ for 1-dB degradation.}$$

The ratio of differential transmission time to channel time constant is the rate at which the propagation time may vary as a result of meteor velocity. This parameter is determined from Fig. 10 by using the station separation and reading the corresponding ratio. For $D = 1500$ km, the ratio if differential transmission time to channel time constant, $\Delta T/\Delta \tau' = 20 \times 10^{-6}$. The variables for the data rate have now been determined. Inserting these variables into Eq. (32) will provide the maximum allowable data rate:

$$\text{Data rate} = \frac{\left(\frac{\text{Time delay}}{\text{Bit width}}\right)}{T\left(\frac{\Delta T}{\Delta \tau'}\right)} = \frac{0.1}{(1.44)\,(20 \times 10^{-6})} = 3500 \text{ bits/s.}$$

Channel Duration—The channel should remain open during the time required for:

- The transit command to travel from the meteor trail to the buoy receiver
- Processing the transit command
- Transmitting the message
- The transit time for the message to reach the meteor trail.

The first and last of these times are

$$t(1,4) = \frac{750 \times 10^3 \text{ m}}{3 \times 10^8 \text{ m/s}} = 250 \times 10^{-5} \text{ s}.$$

For the processing time, it shall be assumed that the formatting and coding efficiency of the message is 50 percent. The requirement to transmit 2000 bits of data per hour is translated into a requirement for transmitting 4000 bits total per hour. The time required to perform this transmission is

$$t_3 = \frac{4000 \text{ bits}}{3500 \text{ bits/s}} = 1.14 \text{ s}.$$

The total transmission time becomes

$$t_T = t_1 + t_2 + t_3 + t_4$$

$$= 0.0025 + 0.101 + 1.14 + 0.0025$$

$$= 1.155 \text{ s}.$$

Channel Opening Rate — Examination of Fig. 7 and Eq. (5) indicates that the optimum transmission time is between 1.5 and 3.0 time constants. From above, a transmission time of 1.155 s and the link time constant $\tau' = 0.72$ s were derived. From Eq. (18b),

$$K = \frac{\text{Transmission time}}{\text{Time constant}} = \frac{1.155}{0.72} = 1.61,$$

which falls within the optimum range. Therefore, only one transmission per hour is required. To provide reliable communications on an hourly basis, diurnal and seasonal variations must be compensated for, as stated before. This can be accomplished by generating a link with 5.5 times the number of channel openings per hour required. Therefore, the mean channel openings for this system is 5.5 per hour.

Receiver Bandwidth — The receiver predetection bandwidth required for this system is a bandwidth equal to twice the data rate plus the doppler bandwidth, plus the bandwidth required to compensate for frequency instability. From Eq. (33),

$$\text{doppler bandwidth } \Delta f = 2f\left(\frac{\Delta T}{\Delta \tau'}\right),$$

$$\Delta f = 2(20 \times 10^{-6})(24 \times 10^6) = 1{,}400 \text{ Hz}.$$

Assume an oscillator stability of ±10 ppm; then

$$\text{Oscillator stability bandwidth} = 2\,(\text{oscillator stability})\,f$$
$$= 2(10 \times 10^{-6})(35 \times 10^{6})$$
$$= 700 \text{ cycles.}$$

$$\text{Receiver bandwidth required} = 2(3500) + 1400 + 700$$
$$= 9100 \text{ cycles.}$$

Path Loss — The path loss in this example is determined in a fashion identical with that shown in the preceding analysis. With the overlap area A already determined, it is possible to obtain the required electron line density q. To do this, we determined the number of channel openings available from a 15,000-km^2 overlap area at a standard electron line density $q = 10^{14}$. Since electron line density is inversely proportional to the desired channel openings, the desired channel openings from the system data and the available channel openings determined from Fig. 8 are entered as a ratio into Eq. (26) to compute the electron line density. Figure 8 shows the number of mean channel openings per hour to be expected for $q = 10^{14}$. With the antenna overlap area of 15,000 km and the station separation of 1500 km, the number of channel openings available for $q = 10^{14}$ is 13.5. The actual value of electron line density required for this link is determined from Eq. (26) as a function of the ratio of the channel openings available to the channel openings desired, as derived in the section on channel opening rate. From Eq. (28), the electron line density,

$$q = \frac{\text{channel openings available}}{\text{channel openings desired}} \times 10^{14} = \left(\frac{13.5}{5.5}\right) \times 10^{14}$$
$$= 2.45 \times 10^{14}.$$

With A and q determined, it is necessary to determine only K, the time-constant factor, in order to determine the path loss. The time-constant factor K is the ratio of the desired transmission time to the link time constant τ as shown in Eq. (18b). With the link time constant as evaluated in the "Data Rate" section, the time constant factor K may be computed. From Eq. (18b), time constant factor

$$K = \frac{\text{transmission time}}{\text{time constant}}$$
$$= \frac{1.155}{0.72} = 1.60.$$

At this point we have evaluated the variables with a functional relationship to the path loss. The next step in the design process is the calculation of the path loss associated with the transmission media. This loss is a function of five variables: electron line density q, f, and station separation D. The path losses associated with each variable are computed and summed, resulting in the total path loss. From Fig. 3 the loss for an equivalent 1000-km link operating at 30 MHz with $q = 2.45 \times 10^{14}$ is determined as 173 dB. This loss must be

scaled by the operating frequency of 35 MHz chosen in the "Frequency" section, which results in

$$L_1 = 30 \log \frac{f}{30} = 30 \log \frac{35}{30} = 2.0 \text{ dB}.$$

An additional modification to the path loss must be considered to provide for nonzero reflection areas and station separations other than 1000 km. The loss modification with respect to these two parameters (A = 15,000 km^2 and D = 1500 km) is taken from Fig. 4 as 4.5 dB. Since the channel path loss increases with channel time, additional losses must be considered for communication time requirements of finite duration. With the time constant factor K already determined as 1.6, the time constant loss is taken from Fig. 7 as 7.0 dB.

The losses computed above are now summed to determine the total path loss. The loss elements being summed are (a) path loss for $q = 2.45 \times 10^{14}$, (b) path loss differential at operating frequency, (c) reflection area and differential station separation loss, and (d) time constant loss. Thus, the total path loss is

$$173 + 2.0 + 4.5 + 7.0 = 186.5 \text{ dB}.$$

Having ascertained the path loss, the transmitter power required to effect this link is determined through use of conventional communication system analysis techniques.

Receiver Sensitivity — The receiver sensitivity is now computed to provide a basis for performing a link calculation. Consideration must be given to the thermal noise as well as extraneous noise in the desired transmission bandwidth. In addition to these factors, the signal-to-noise degradation resulting from propagation time variation and the signal-to-noise ratio required to obtain the desired error rate must be considered. To determine the thermal noise at the receiver input, we add the thermal noise in a one-cycle bandwidth to the bandwidth factor that corresponds to the required 9100-cycle bandwidth determined in the "Channel Opening Rate" section.

Thermal noise for a 1-Hz bandwidth	−174 dBm
Bandwidth factor for a 9100-cycle bandwidth	39.5 dB
Thermal noise at receiver	−134.5 dBm

In addition to the thermal noise, man-made noise is found to be of greatest magnitude [3]. This noise is found to be of 15 dB greater magnitude than the thermal noise at 35 MHz. To compute the receiver noise, we add the excess man-made noise to the thermal noise.

Thermal noise at receiver	−134.5 dBm
Man-made noise above thermal (quiet location)	15 dB
Total noise at receiver input	−119.5 dBm

The signal requirements at the receiver will be a level somewhat in excess of the noise, depending upon the type of modulation employed and the error rate to be tolerated [4]. Because of the path length variability and the desire to maintain system simplicity, a noncoherent frequency-shift-key-modulated carrier is chosen for transmission. A 10^{-14} error

rate is selected as being acceptable for this link. A 13-dB signal-to-noise ratio is required to achieve this performance. The minimum signal strength then required at the receiver is obtained by adding the required signal-to-noise ratio to the total noise in the receiver.

Total noise at receiver input	−119.5 dBm
Signal-to-noise ratio required	13 dB
Minimum signal required at receiver	−106.5 dBm

As determined in the "Data Rate" section, a signal-to-noise ratio degradation of 1 dB can be expected because of the propagation time variability of the meteor link. Maintaining the desired signal-to-noise ratio as this propagation time varies requires that this degradation level be added to the minimum signal required at the receiver.

Minimum signal required at receiver	−106.5 dBm
Signal degradation from propagation path variation	1 dB
Receiver sensitivity	−105.5 dBm

With the receiver sensitivity determined in this paragraph and the path loss computed in the previous paragraph, the link calculation is performed to determine the transmitter power required.

Link Calculation—The purpose of this section is to determine the remaining unknown system parameter, transmitter power, which we achieve by working back from the receiver to the transmitter. The field strength in dBm required at the receiver is determined by subtracting the base station receiver attenna gain in decibels as selected in the "Base Station Antenna" section from the receiver sensitivity in dBm.

Sensitivity	−105.5 dBm
Receiver antenna gain	24 dB
Receiver field strength	−129.5 dBm

With the receiver field strength and the total path loss computed above, the transmitter ERP may be determined. To this end, the receiver field strength is added to the total path loss.

Receiver field strength	−129.5 dBm
Total path loss	186.5 dB
Transmitter ERP	57.0 dBm

To determine the actual transmitter power required, we need only to subtract the transmitter antenna gain from the transmitter ERP.

Transmitter ERP	57.0 dBm
Transmitter antenna gain	5.0 dB
Transmitter power	52.0 dBm

52 dBm = 160 W.

The result of this computation indicates that a system utilizing a relatively simple remote station and only a moderate installation for the base station can effectively communicate over considerable distances.

System Parameters—The foregoing parameter selections and computations result in a system design that can be used to effect the desired link. The system parameters derived in this example are

Receiver sensitivity	−105.5	dBm
Transmitter power	52.0	dBm
Station separation	1500	km
Buoy antenna gain	5.0	dB
Base antenna gain	24.0	dB
Mean channel openings	5.5	per hour
Link duration	1.155	s
Frequency	35.0	MHz

SUMMARY AND CONCLUSIONS

The system analyses performed using the functional relationships derived indicate that effective over-the-horizon communications can be realized with a modest equipment suite. This technique is most applicable where minimum data throughput and non-real-time data transmissions are required. Advantages of long range, low peak transmitter power, and equipment simplicity make this technology a candidate for numerous remote manned and automated sensing installations.

Meteor incidence in earth's atmosphere is presented as a natural phenomenon that can be exploited for communications propagation. The transmission equations for both the underdense and overdense meteor-burst conditions are presented for link factor functional derivation. Relationships are derived for system analysis from factors including communication equipment functions, propagation characteristics, and physical considerations. Of significant interest are channel occurrence and duration relationships as well as antenna requirements, data rate limitations, and transmission detectability. The value of the derived relationships is illustrated by examples of systems analysis and the presentation of a link design procedure.

The simplifying assumptions made in these derivations are numerous, but some of particular interest are indicated. These include the assumption of a uniform statistical distribution for the seasonal and diurnal meteor incidence variation, the neglect of the zenith cusp in usable meteor trail incidence, and the neglect of cross polarization in the phenomenon of meteor ionization trail reflection. These considerations, in addition to the other assumptions made, provide further avenues for refining meteor-burst technology in subsequent investigations. Since the functional relationships as presented were conservatively derived, subsequent analytical refinements can be expected to reveal additional meteor-burst link advantages.

The foregoing discussion presents functional relationships of the major parameters associated with meteor-burst communications technology. From these relationships an approach for the analysis and synthesis of meteor-burst communications links is established. Examples are provided which employ the procedures generated and illustrate their use in the link design and analysis procedure. The sophistication that results from the refinement of functional relationships can be incorporated into a computer design format that can be used to extend the accuracy and ease of meteor-burst link design and analysis.

ACKNOWLEDGMENTS

The writer gratefully acknowledges a critical review of the manuscript by Dr. J. M. Norris. In addition, thanks are due to Mrs. M. Koncen for her dedicated efforts in typing the manuscript and H. W. Zwack for his support and guidance throughout this period.

REFERENCES

1. K. Davies, "Ionospheric Radio Propagation," NBS Monograph 80, p. 355, April 1, 1965.
2. P.A. Forsyth, E.L. Vogan, D.R. Hansen, and C.O. Hines, "The Principles of JANET—A Meteor-Burst Communication System," *Proc. IRE* 45, 1642—1657 (Dec. 1957).
3. ITT Corporation, *Reference Data for Radio Engineers*, Howard W. Sams Co., New York, 1968, pp. 27—33.
4. M. Schwartz, R.W. Bennet, and S. Stein, *Communication Systems and Techniques*, McGraw-Hill, New York, 1966, p. 299.

BIBLIOGRAPHY

"Remote Instrument Communications System," Ball Bros. Research Corporation, Boulder, CO 80302.

Ball Bros. Research Corporation, TR71-30, Boulder, CO 80302.

Ball Bros. Research Corporation, TR71-37, Boulder, CO 80302.

P.J. Bartholomé, "The STC Meteor-Burst System," SHAPE Technical Centre Tech. Memo. TM-156, Feb. 1967 (AD 811317).

P.J. Bartholomé, "Results Obtained with the STC Meteor-Burst Communication System," SHAPE Technical Centre Tech. Memo. TM-165, July 1967 (AD 818053).

H.E. Chubb, H.L. Heibeck, and C.G. Wilhelm, "A Meteor Scatter Communications System Using Digital Storage," NFL Report 1033, U.S. Navy Electronics Laboratory, San Diego, CA, 1961.

V.R. Eshleman, and L.A. Manning, "Radio Communication by Scattering from Meteoric Ionization," *Proc. IRE* 42, 530—536 (Mar. 1954).

F.A. Gunther, "Tropospheric Scatter Communications—Past, Present, and Future," *IEEE Spectrum* 3 (No. 9), 79—100 (Sept. 1966).

J.L. Heritage, J.E. Bickel, and C.P. Kugel, "Meteor Burst Communication in Minimum Essential Emergency Communications Network (MEECN)," NELC Working Paper prepared for DCA, MEECN Systems Office (Code 960), Oct. 1976.

D.I. Himes and W. Marshall, "Study of Meteor Trail Propagation and Meteor Burst Communications Systems," Report for Avionics Equipment Laboratory, ITT Laboratories, Nutley, NJ (date unknown).

L.E. Keltner, D.J. Marihart, and D.N. March, "Meteor Burst Communications System for Hydromet Data Acquisition," International Communications Conference, pp. 9—24 through 9—29, 1973.

DEPARTMENT OF THE NAVY

NAVAL RESEARCH LABORATORY
Washington, D.C. 20375

OFFICIAL BUSINESS
PENALTY FOR PRIVATE USE, $300
THIRD CLASS MAIL

POSTAGE AND FEES PAID
DEPARTMENT OF THE NAVY
DoD-316